7-1-2019

Exact Analytical Formula for the Excess Noise Factor for Mixed Carrier Injection Avalanche Photodiodes

Md. Mottaleb Hossain
University of New Mexico

John P.R. David
University of Sheffield

Majeed M. Hayat
Marquette University, majeed.hayat@marquette.edu

Journal of Lightwave Technology, Vol. 37, No. 13 (July 1, 2019): 3315-3323. DOI.

Exact Analytical Formula for the Excess Noise Factor for Mixed Carrier Injection Avalanche Photodiodes

Md. Mottaleb Hossain
Center for High Technology Materials and the Department of Electrical and Computer Engineering, University of New Mexico, Albuquerque, NM
John P. R. David
Electronic and Electrical Engineering Department, University of Sheffield, Sheffield, U.K.
Majeed M. Hayat
Center for High Technology Materials and the Department of Electrical and Computer Engineering, University of New Mexico, Albuquerque, NM

Abstract:

The well-known analytical formula for the excess noise factor associated with avalanche photodiodes (APDs), developed by R. J. McIntyre in 1966, assumes the injection of either an electron or a hole at the edge of the APD's avalanche region. This formula is based on the statistics of the probabilities of carriers gaining and losing energy subject to high electric fields. However, this analytical formula, is not applicable in cases when photons are absorbed inside the avalanche region (even though the physics of the high field transport remains the same), and its use may severely underestimate or overestimate the actual excess noise factor depending on the absorption profile and the hole-to-electron ionization coefficient ratio, k. Here, an easy-to-use exact analytical formula is derived for the excess noise factor of APDs while taking into account a mixed-carrier initiated avalanche multiplication process, which is triggered by a parent electron-hole pair at an arbitrarily specified location within the multiplication region. The derivation relies on analytically solving a special case of a previously reported recursive integral equations [Hayat et al., IEEE Trans. Electron Devices, vol. 39, no. 3, pp. 546-552, Mar. 1992.], and the result matches the formula reported by McIntyre in 1999 using a different and limited technique. In addition, an expression for the excess noise factor is presented in the case when the location of the parent electron-hole pair within the multiplication region obeys an arbitrary exponential distribution. The results show that in contrast to the case of edge parent-electron injection, when mixed injection is allowed even a small level of hole ionization (e.g., small k ~ 0.0001) causes the excess noise factor to increase dramatically, depending on the absorption profile as it ranges from narrow to flat within the multiplication region. The theoretical results are validated against experimental results for Si APDs.

SECTION I. Introduction

Avalanche photodiodes (APDs), with their high internal gain, are widely used in optical communication systems due to the improvement they offer to the receiver's signal-to-noise ratio (SNR). The receiver performance is strongly dependent on the APDs mean gain (*M*) and the excess noise factor (*F*), which represents the random fluctuations in the gain. Thus, availability of analytical expressions for *M* and *F* is important for calculating the SNR as well as the bit-error probability in optical receivers [1]. The quantities *M* and *F* are commonly related to the hole-to-electron ionization coefficient ratio, *k*, as expressed in McIntyre's original theory [2] dating back to 1966. The *F* value is at a minimum for materials with a small value of *k* and electron edge injection (or very large *k* for hole edge injection), namely when a parent electron (hole) is injected into the appropriate edge of the multiplication region, resulting in a chain of impact ionizations. In reality, however, mixed-carrier injection can occur in the multiplication region (MR), whereas photons are absorbed inside the MR [2]. Such scenario results in a parent electron-hole pair inside the MR initiating the avalanche multiplication process, where each parent carrier independently and individually creates its own chain of impact ionizations.

It turns out that mixed injection plays an important role in the behavior of *F* as a function of *M*, as originally pointed out by Webb *et al.* in [3]. For example, we will show in this paper even when *k* is very low (~0.0001), *F* begins to increase dramatically beyond a certain threshold value of *M* if mixed injection is allowed. Moreover, the mean gain threshold at which *F* becomes large is determined as a function of the location of mixed injection and *k*. The main contribution of this paper is to develop an exact analytical formula for *F* in the case of mixed-injection avalanche multiplication process. Consequently, depending on the photon absorption profile within the MR, photogenerated carriers within the MR contribute collectively to mixed-injection multiplication in a distributed fashion. Thus, for a given APD structure, *M* and *F* may actually depend indirectly on the wavelength of light. Note that the small values of *k* of 0.01 or lower are important from a practical standpoint as there are several bulk materials that exhibit this type of mixed-injection behavior including Si [4], [5], InAs [6], and AlAsSb [7]. In addition, high values of *k* (>0.1) are also important for submicron

multiplication regions (e.g., Si *pn*-junction APDs), where the very high electric fields (>255 kV/cm) cause an increase in the *k* value [8], [9].

Although McIntyre developed closed-form expressions for the mean gain and noise spectral density in the case of mixed injection [2], he did not offer a formulation of the excess noise factor under distributed-injection case. In 1992, Hayat *et al.* formulated an analytical model [10] for avalanche multiplication that allowed the determination of the excess noise factor in the case of mixed injection while also incorporating the effect of dead space, which is the minimum distance a carrier must travel after an impact ionization before it may effect another ionization. In 2017, Hossain *et al.* used the numerical approach to further calculate the excess noise factor for Si APDs in the case of distributed mixed injection [9], where the photon absorption profile within the MR was taken into account. Experiments have also shown the wavelength dependence of the excess-noise factor; moreover, good agreement between numerical solutions of the analytical model and experiments on the role of mixed injection has been shown [5], [8]–[9][10][11][12]. The experiments and the numerically calculated *F* under mixed injection were also compared with that calculated using the McIntyre's formula [2], which assumes edge injection. For example, the comparison showed that McIntyre's *F* significantly overestimated the measured *F* for CMOS APDs [8]. Other examples are low doped (i.e., thick) CMOS APDs [13], where the excess noise factors were calculated using the classical McIntyre's formula. As shown in Fig. 3 in [13], the classical noise can be easily calculated with pure electrons and holes; however, this is not the case when a distributed carrier injection profile is taken into consideration. The calculated *F* does not lie half-way between the two extremes; moreover, the correct answer cannot be calculated from the excess noise factors associated with pure electron and pure hole injections. Therefore, the aforementioned results emphasize the need for a distributed-injection formula for *F* in practice.

To the best of our knowledge, there is no analytical formula for the excess noise factor in the case of distributed injection APDs taking into account photon absorption profile. The most relevant work relevant to a closed-form formula for the excess noise factor in the case of mixed injection is the work of Hayat *et al.* [14]. The article shows exact analytical expressions for *M* and *F* under edge injection by finding an exact analytical solution to the recursive integral equations [10] that characterize the first and second moments of the populations of electrons and holes under mixed injection. This approach is termed the characteristic method (CM). The article in [14] did not provide explicit formulas for *F* under mixed injection. Note that McIntyre provided a mixed injection formula for *F* [15] following the derivation in [2] using a different approach, which is limited to the case when dead space is ignored.

In this work, we revisit the CM approach to rigorously derive an exact analytical formula of the excess noise factor for mixed carrier injection with zero dead space. The novel probabilistic and direct derivation given here in (21) has been not published anywhere in its form. The analytically calculated *F* is compared with McIntyre's 1999 formula [15]and that calculated numerically using dead-space multiplication theory (DSMT) [10], and agreement is shown. In addition, expressions for the analytical mean gain and excess noise factor are presented while taking into account different absorption profiles using an exponential decay function. Moreover, previously reported *F* for the P+/N-well CMOS APD [9] are compared with that analytically calculated under mixed injection case and good agreement is shown.

SECTION II. Analytical Formulation of the Mixed-Injection F

Consider the multiplication region of an APD extended from $x = 0$ to $x = W$, where W is the avalanche multiplication-region width. It is further assumed that the avalanche multiplication process is initiated by a photogenerated electron-hole pair within the MR. Now consider a parent electron and a parent hole that are located at position *x*within the multiplication region. Electrons are assumed to travel in the positive *x*-direction at their saturation velocity under the influence of electric field and they are capable of impact ionizing with an

ionization coefficient, α. Similarly, holes travel in the negative x-direction and are capable of impact ionizing with an ionization coefficient, β. This avalanche process produces a net stochastic gain, $G(x)$, when all the carriers have exited the MR; this quantity is the total number of electron-hole pairs generated as a result of a single parent electron-hole pair, located at x, initiating the multiplication process. Next, we analyze the statistics of $G(x)$.

Following Hayat *et al*. [10], define $Z(x)$ as the random sum of electrons and holes produced by an electron, including the initiating parent electron. Similarly, let $Y(x)$ be the random number of all electrons and holes produced by the hole and its offsprings, including the initiating parent hole. Note that $Z(W) = 1$ and $Y(0) = 1$. Moreover, $G(x) = \frac{1}{2}[Z(x) + Y(x)]$. Now consider the averages $z(x) = \langle Z(x) \rangle$ and $y(x) = \langle Y(x) \rangle$, which are the means of $Z(x)$ and $Y(x)$, respectively; similarly, $z_2(x) = \langle Z^2(x) \rangle$ and $y_2(x) = \langle Y^2(x) \rangle$ are the second moments of $Z(x)$ and $Y(x)$, respectively. Here, the bracket denotes ensemble average. The mean of $G(x)$ is obtained from the quantities of $z(x)$ and $y(x)$:

$$M(x) = \langle G(x) \rangle = \frac{1}{2}[z(x) + y(x)]. \quad (1)$$

On the other hand, the second moment of the gain in the case of a mixed-carrier initiated avalanche is given by

$$\langle G^2(x) \geq \frac{1}{4}[z_2(x) + 2z(x)y(x) + y_2(x)]. \quad (2)$$

Finally, in this paper, we define the mixed-injection excess-noise factor, $F(x)$, as follows:

$$F(x) = \frac{\langle G^2(x) \rangle}{\langle G(x) \rangle^2}. \quad (3)$$

The above equations require knowledge of the ionization coefficients for electrons (α) and holes (β), respectively. The electric-field dependent ionization coefficients are widely modeled [9], [15]–[16][17][18] using Chynoweth's formula [19] and the expressions are given by

$$\alpha(E) = A_e exp[-(\frac{B_e}{E})^{m_e}] \quad (4a)$$

and

$$\beta(E) = A_h exp[-(\frac{B_h}{E})^{m_h}], \quad (4b)$$

where E is the electric field and the A, B, and m are material-dependent parameters, and they are chosen from material specific experimental and fitted data [9], [15]–[16][17][18]. The electric field within the MR in conjunction with the ionization coefficients, $\alpha$and β, are used in (3) to predict the injection-position dependent excess-noise factor under mixed injection case.

A. Formula for Mixed-Injection Mean Gain

In order to obtain an exact analytical formula for $M(x)$, we solve the recursive integral equations from the DSMT model [10] with zero dead space to obtain the quantities $z(x)$ and $y(x)$ under mixed injection. The recursive integral equations for z(x) and $y(x)$ are equations (14) and (15) in [10]:

For $0 \leq x \leq w$,

$$\begin{aligned} z(x) &= [1 - (1 - e^{-\alpha(W-x)})u(W - x)] \\ &\quad + \int_x^W [2z(\xi) + y(\xi)]\, \alpha e^{-\alpha(\xi - x)} u(\xi - x) d\xi \quad (5a) \\ y(x) &= [1 - (1 - e^{-\beta x})u(x)] \\ &\quad + \int_0^x [2y(\xi) + z(\xi)]\, \beta e^{-\beta(x-\xi)} u(x - \xi) d\xi, \quad (5b) \end{aligned}$$

where $u(x) = 1$ for $x \geq 0$, and 0 otherwise.

Upon differentiation with respect to *x* and simple back substitution, the differential forms of the above integral equations are

$z'(x) + \alpha[z(x) + y(x)] = 0$ (6a)

View Source and

$y'(x) - \beta[z(x) + y(x)] = 0$,(6b)

with the boundary conditions, $z(w) = 1$ and $y(0) = 1$. The approach we undertake to solve for *z*(*x*) and *y*(*x*) exactly is based on proposing exponential-form solutions, as done in [10]. The desired exponents are then found by substituting these assumed exponential forms in (6a) and (6b), and obtaining an algebraic *characteristics equation*characterizing the exponents that result in self consistency in (6a) and (6b). More precisely, the general structure of the solution is a superposition of terms of the form

$z(x) = c_1 e^{rx}$ (7a)

and

$y(x) = c_2 e^{rx}$, (7b)

where c_1 and c_2 are the unknown coefficients and *r* is a solution to the characteristic equation.

After we substitute these general solutions from (7a) and (7b) into (6a) and (6b), respectively, we obtain the matrix equation

$$\begin{bmatrix} (r+\alpha) & \alpha \\ -\beta & (r-\beta) \end{bmatrix} \begin{bmatrix} c_1 \\ c_2 \end{bmatrix} = \begin{bmatrix} 0 \\ 0 \end{bmatrix} \text{..(8)}$$

For a nontrivial (i.e., nonzero) solution to c_1 and c_2 in (8), we require that the matrix above to be singular (its determinant must be zero), which results in the characteristic equation characterizing *r*:

$(r + \alpha)(r - \beta) + \alpha\beta = 0$. (9)

We begin by considering the case when electron and hole ionizations are unequal (*k* ≠ 1), in which case (9) has two roots: $r_1 = 0$and $r_1 \equiv r = \beta - \alpha \neq 0$. The general solution in this case becomes

$z(x) = c_1 + c_1' e^{rx}$ (10a)

and

$y(x) = c_2 + c_2' e^{rx}$..(10b)

Upon substituting the general solutions from (10a) and (10b) into (6a) and applying the boundary conditions $z(w) = y(0) = 1$, we obtain a system of four linear equations with four unknown coefficients c_1, c_1', c_2, and $c_2'$with *r*. After some algebra, the unknown coefficients are determined and the first moments of $z(x)$ and $y(x)$are obtained as follows:

$z(x) = \frac{(r+\alpha+\alpha e^{rw})-2\alpha e^{rx}}{(r+\alpha-\alpha e^{rw})}$ (11a)

and

$y(x) = \frac{-(r+\alpha+\alpha e^{rw})+2(r+\alpha)e^{rx}}{(r+\alpha-\alpha e^{rw})}$. (11b)

Next, the analytical expression for the mean-gain for a mixed-carrier initiated avalanche, $M(x)$, is obtained from the quantities of z(x) and $y(x)$ using (1). Specifically, we maintain that

$$M(x) = \frac{re^{rx}}{r+\alpha-\alpha e^{rw}} = \frac{(\beta-\alpha)e^{(\beta-\alpha)x}}{\beta-\alpha e^{(\beta-\alpha)w}}; \text{ (12a)}$$

or equivalently,

$$M(x) = \frac{(1-k)e^{-\alpha(1-k)x}}{e^{-\alpha(1-k)w}-k}, \text{ (12b)}$$

where $k = \frac{\beta}{\alpha}$. This expression was previously derived by McIntyre (equation (5) in [2]) using a different method.

In addition, the expression for ionization parameter, αw, in terms of k, $M(x)$ and the mixed-injection location (x/w) within the MR is derived as

$$\alpha w = \ln\left(\frac{e^{(1-k)}}{k} - \frac{(1-k)e^{(1-k)(\frac{x}{w})}}{kM(x)}\right). \text{ (13a)}$$

Recall that for an APD device, avalanche breakdown occurs for a value of ionization parameter for which the mean gain $M(x)$ is infinite. In this case, (13a) becomes

$$(\alpha w)_b = \ln\frac{e^{(1-k)}}{k}. \text{ (13b)}$$

Hence, the breakdown condition is independent of the location of the parent injection, x.

For the case of electron injection $\beta < \alpha$, hence $k < 1$, and $x = 0$), (12) collapses to the well-known McIntyre's classical mean-gain formula in the case of edge electron-injection [2]:

$$M_e = M(0) = \frac{1-k}{e^{-\alpha(1-k)w}-k}. \text{ (14a)}$$

Similarly, for hole injection ($\beta > \alpha$, equivalently $k > 1$and $x = w$), (12) becomes

$$M_h = M(w) = \frac{1-\frac{1}{k}}{e^{-\beta(1-\frac{1}{k})w}-\frac{1}{k}}. \text{ (14b)}$$

Next, consider the case $k = 0$ in (14a) or $k = \infty$ in (14b), and obtain

$$M_e = e^{\alpha w} \text{ (15a)}$$

and

$$M_h = e^{\beta w}. \text{ (15b)}$$

Similarly, to consider the case when $k = 1$ in (12) and (14), we take the limit as $k \to 0$ (or $k \to \infty$) and obtain the familiar position-independent formula

$$M(x) = \frac{1}{1-\alpha w}. \text{ (16)}$$

The special-case expressions in (15) and (16) are the well-known McIntyre formulas (equations (21) and (24) in [20]).

We note that the approach followed in this paper to obtain the mixed-injection mean gain is intrinsically different from that followed by McIntyre. Unlike McIntyre's approach, the approach here lends itself to a solution of the mixed-injection excess noise factor, as described next.

B. Formula for Mixed-Injection Excess-Noise Factor

In order to obtain an exact analytical formula for *F*(*x*), we solve the recursive integral equations from the DSMT model [10] with zero dead space to obtain the second moments of electrons and holes, $z_2(x)$ and $y_2(x)$, respectively, under mixed injection. The recursive integral equations for the second moments of *Z*(*x*) and *Y*(*x*) are equations (22) and (23) in [10], and they are expressed below:

For $0 \le x \le w$,

$$\begin{aligned} z_2(x) &= [1-(1-e^{-\alpha(W-x)})u(W-x)] \\ &+ \int_x^W [2z_2(\xi)+y_2(\xi)+4z(\xi)y(\xi)+2z^2(\xi)] \\ &\times \alpha e^{-\alpha(\xi-x)}u(\xi-x)d\xi \end{aligned} \quad (17a)$$

and

$$\begin{aligned} y_2(x) &= [1-(1-e^{-\beta x})u(x)] \\ &+ \int_0^x [2y_2(\xi)+z_2(\xi)+4z(\xi)y(\xi)+2y^2(\xi)] \\ &\times \beta e^{-\beta(x-\xi)}u(x-\xi)d\xi. \end{aligned} \quad (17b)$$

The differential forms of the above recurrence equations are

$$z_2'(x)+\alpha[z_2(x)+y_2(x)] = -2\alpha z(x)(2y(x)+z(x)) \quad (18a)$$

and

$$y_2'(x)-\beta[z_2(x)+y_2(x)] = 2\beta y(x)(2z(x)+y(x)),, \quad (18b)$$

with the boundary conditions, $z_2(w) = 1$and $y_2(0) = 1$. Note that the right-hand sides of (18a) and (18b) are explicitly determined by substituting the previously derived expressions given by (11a) and (11b). To solve the above inhomogeneous differential equations exactly, we assume a general solution (combination of complementary and particular solution) to the unknown functions $z_2(x)$and $y_2(x)$ in the form

$$z_2(x) = p_1e^{rx}+p_2e^{2rx}+p_3xe^{rx}+p_4x+p_5 \quad (19a)$$

and

$$y_2(x) = q_1e^{rx}+q_2e^{2rx}+q_3xe^{rx}+q_4x+q_5.. \quad (19b)$$

The exponent *r* turns out to satisfy the same characteristic equation as in (9). Upon substituting the proposed forms from (19a) and (19b) into (18a) and (18b) and applying boundary conditions $z_2(w) = y_2(0) = 1$, we obtain a system of twelve linear equations with ten unknown coefficients p_1, p_2, p_3, p_4, p_5, q_1, q_2, q_3, q_4, and q_5. After some algebra, the unknown coefficients are determined and second moments of $z_2(x)$ and $y_2(x)$are obtained. The details of the calculations are omitted.

Finally, the analytical expression for the excess noise factor for a mixed-carrier initiated avalanche, *F*(*x*), is obtained from the quantities of *z*(*x*), *y*(*x*), $z_2(x)$and $y_2(x)$as follows:

$$F(x) = \frac{<G^2(x)>}{<G(x)>^2} = \frac{\frac{1}{4}[z_2(x)+2z(x)y(x)+y_2(x)]}{(\frac{1}{2}[z(x)+y(x)])^2}. \quad (20a)$$

Hence, upon substituting the exact expressions for *z*(*x*), *y*(*x*), $z_2(x)$and $y_2(x)$ in (20a) we obtain

$$F(x) = 2-\{\frac{e^{-2\alpha(1-k)w}-k}{e^{-\alpha(1-k)w}-k}\}e^{\alpha(1-k)x}, \quad (20b)$$

where $k = \frac{\beta}{\alpha}$ and $r = \beta - \alpha \neq 0$.

The excess noise factor, $F(x)$, can also be represented in terms of mean gain, $M(x)$, and k. More precisely,

$$F(x) = kM(x)e^{2\alpha(1-k)x} + 2(1 - ke^{\alpha(1-k)x}) - \frac{1}{M(x)}(1-k). \quad (21)$$

The formula in (20b) (or (21)) is the generalization of McIntyre's formula for the excess noise factor to mixed injection and it constitutes the first major contribution of this paper. Note that an equivalent form of (20b) (or (21)) was previously reported by McIntyre (equation (4) in [15]), following equation (13) in [2], using a different method. We believe that the rigorous probabilistic derivation given here is both simpler to follow and more direct than the methodology reported in deriving equation (13) in [2].

For the case of electron injection ($\beta < \alpha$, hence $k < 1$, and $x = 0$), (21) collapses to the well-known McIntyre's [2] formula:

$$F_e = F(0) = kM_e + (2 - \frac{1}{M_e})(1-k). \quad (22a)$$

Similarly, for hole injection ($\beta < \alpha$, equivalently $k < 1$, and $x = w$), (21) becomes

$$F_h = F(w) = \frac{M_h}{k} + (2 - \frac{1}{M_h})(1 - \frac{1}{k}). \quad (22b)$$

Next, consider the case when $k = 0$ in (22a) or $k = \infty$ in (22b). In these cases, we obtain

$$F_e = 2 - \frac{1}{M_e} \quad (23a)$$

and

$$F_h = 2 - \frac{1}{M_h}. \quad (23b)$$

To address the case when $k = 1$, we take the limit as $k \to 1$ in (21) and obtain the familiar formula

$$F(x) = M(x) = \frac{1}{1-\alpha w}. \quad (24)$$

The special-case expressions in (23) and (24) are those as given by (19) and (22) in [20].

C. Analytical Expressions for Distributed Mixed-Injection M and F With an Exponential Decay Function

Ideally, pure electron (e.g., for Si with low k) or pure hole (e.g., for InP with high k) edge-injection yields the lowest value of F. This can be seen from the expression for $F(x)$ in (21). However, depending on the photon absorption profile inside the MR, photogenerated carriers within the MR also contribute collectively to the mixed-injection multiplication in a distributed fashion. Thus, for a given APD structure, M and F actually depend indirectly on the wavelength of light. In this regard, we present analytical expressions for M and F while taking into account different absorption profiles with an exponential decay function within the MR.

Consider an incident photon that is absorbed in the multiplication region $(0 \leq x \leq w)$with probability p_m. The generation rate for mixed carrier injection is proportional to $e^{-\alpha' x}$, where α' is the material absorption coefficient. When the absorption profile is normalized by $p_m / \int_0^w e^{-\alpha' x} dx$, we obtain the probability density function (pdf) of the location of absorption within the MR, namely $g(x) = \frac{\alpha' e^{-\alpha' x}}{1 - e^{-\alpha' w}}$.

The mean gain for the mixed-carrier initiated avalanche, $M_a =< G_a >$, is obtained from the quantities $z(x)$ and $y(x)$ while taking into account the absorption profile within the MR. More precisely,

$$M_a = \int_0^w \frac{1}{2}[z(x) + y(x)]g(x)dx \text{ ..(25)}$$

By inserting the values of $z(x)$ and $y(x)$ into (25), we obtain the following analytical expression for the distributed injection mean gain:

$$M_a = \frac{\alpha'(1-k)(e^{(-(1-k)\alpha-\alpha')w}-1)}{(e^{-\alpha(1-k)w}-k)(1-e^{-\alpha' w})(-\alpha(1-k)-\alpha')} \text{ .(26)}$$

Similarly, the second moment of mean avalanche gain for the mixed-carrier initiated avalanche, <G2a>, is obtained from the quantities $z(x)$, $y(x)$, $z_2(x)$, and $y_2(x)$ while taking into account the absorption profile within the MR:

$$< G_a^2 >= \int_0^w \frac{1}{4}[z_2(x) + 2z(x)y(x) + y_2(x)]g(x)dx \text{ .(27)}$$

Moreover, the distributed-injection excess noise factor, $F_a(x)$, with absorption profile is expressed as

$$F_a = \frac{<G_a^2>}{{M_a}^2} \text{ ,(28)}$$

which reduces to the formula as shown at the bottom of this page.

$$F_a = \frac{\frac{\alpha'}{1-e^{-\alpha' w}}\left[\left\{\frac{2\left(e^{(-2\alpha(1-k)-\alpha')w}-1\right)}{-2\alpha(1-k)-\alpha'}\right\} - \left\{\frac{e^{-2\alpha(1-k)w}-k}{e^{-\alpha(1-k)w}-k}\right\}\left\{\frac{\left(1-e^{(-\alpha(1-k)-\alpha')w}\right)}{\alpha(1-k)+\alpha'}\right\}\right]}{\left\{\frac{\alpha'}{1-e^{-\alpha' w}}\frac{\left(e^{(-\alpha(1-k)-\alpha')w}-1\right)}{-\alpha(1-k)-\alpha'}\right\}^2}$$

The formula in (29) is the generalization of McIntyre's formula for the excess noise factor to distributed injection and it constitutes the second major contribution of this paper.

SECTION III. Results

The behavior of *F*(*x*) as a function of *M*(*x*) is shown in Fig. 1, which results from the exact analytical formula shown in (21). Six cases of *k* and three cases of relative mixed-injection parameter (*x*/*w*) are considered. The *k* values are 0.0001, 0.001, 0.01, 0.1, 0.5, and 0.9, and the *x*/*w* values are 0, 0.5 and 1. As expected, the excess noise factor shows strong dependence on mixed-injection location for different values of *k*. In general, the excess noise factor is at a minimum for materials with a small value of *k* and edge electron-injection (or very large *k* for edge hole-injection), namely when the parent electron (hole) is injected at the appropriate edge of the multiplication region. However, in contrast to the case of edge parent-electron injection, even when *k* is very low, i.e., *k* = 0.0001, the excess-noise factor behavior shows dramatic increase with the mixed injection location (*x*/*w* ranging from 0 to 1) within the MR, as seen from Fig. 1. It turns out that mixed injection plays an important role in the behavior of *F*(*x*) as a function of *M*(*x*) as well as injection location and *k* values.

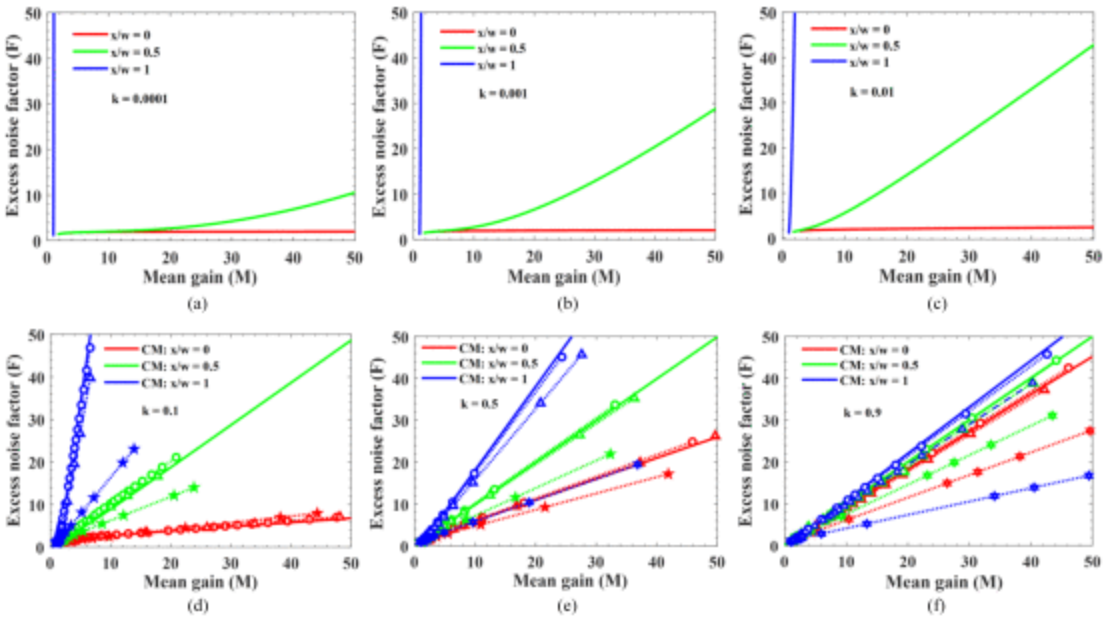

Fig. 1. Excess-noise factor, $F(x)$, as a function of mean gain, $M(x)$. Six cases of hole-to-electron ionization coefficient ratio (k) and three cases of relative mixed injection parameter (x/w) are considered. The k values are 0.0001, 0.001, 0.01, 0.1, 0.5, and 0.9 and x/w values are 0, 0.5 and 1. Excess noise factor calculated using CM approach is compared with that calculated using ENM for k = 0.1, k = 0.5 and k = 0.9, respectively. For ENM, the values of normalized dead space (d/w) are chosen to be 0, 0.01, and 0.1 and are represented by "O", "Δ", and "☆", respectively. In addition, red, green, and blue lines represent relative mixed injection parameter (x/w) with the values of 0, 0.5 and 1, respectively.

For validation purposes, the excess noise factor calculated using the formula in (21) is also compared with that calculated using exact numerical method (ENM) [10] for $k$values of 0.1, 0.5 and 0.9, respectively (see Fig. 1); the good agreement between the two approaches is evident.

In summary, the excess noise factor increases dramatically with the mean gain when mixed injection is allowed within the MR. More precisely, $F(x)$ increases with the location of the mixed injection and k. For example, F increases by a factor of 1.4 at M = 20 for k = 0.0001 when edge injection is replaced by mixed-injection at x/w = 0.5. In addition, even when k is very low (~0.0001), F begins to increase dramatically beyond a certain threshold value of M = 10 when mixed injection is allowed. Moreover, the mean gain threshold at which F becomes large is determined as a function of the location of mixed injection and k. The results show that relying on the k value alone, as we were taught by McIntyre's theory, can be very misleading when mixed injection is a factor.

The pdf, $g(x)$, of the photon absorption location as a function of absorption depth (x) is shown in Fig. 2. The exponential absorption profiles are arbitrarily chosen from narrow to flat, based on the α' values from 10 to 0.01. The behavior of the excess noise factor as a function of mean gain for different absorption profiles is shown in Fig. 3, which results from the exact analytical formulas shown in (26) and (29). Six cases of k and four cases of absorption profiles are considered. In addition, McIntyre's k lines (i.e., x/w = 0) are shown using the dotted lines with k assuming the values of 0.0001, 0.001, 0.01, and 0.1 to 1 with an increment of 0.1.

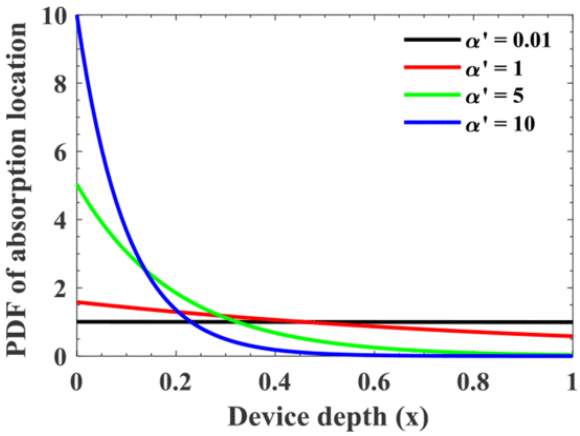

Fig. 2. Probability density function (PDF) of the photon absorption location as a function of the absorption location (*x*) for different absorption coefficient (*α'*) from flat to narrow with an exponential decay function.

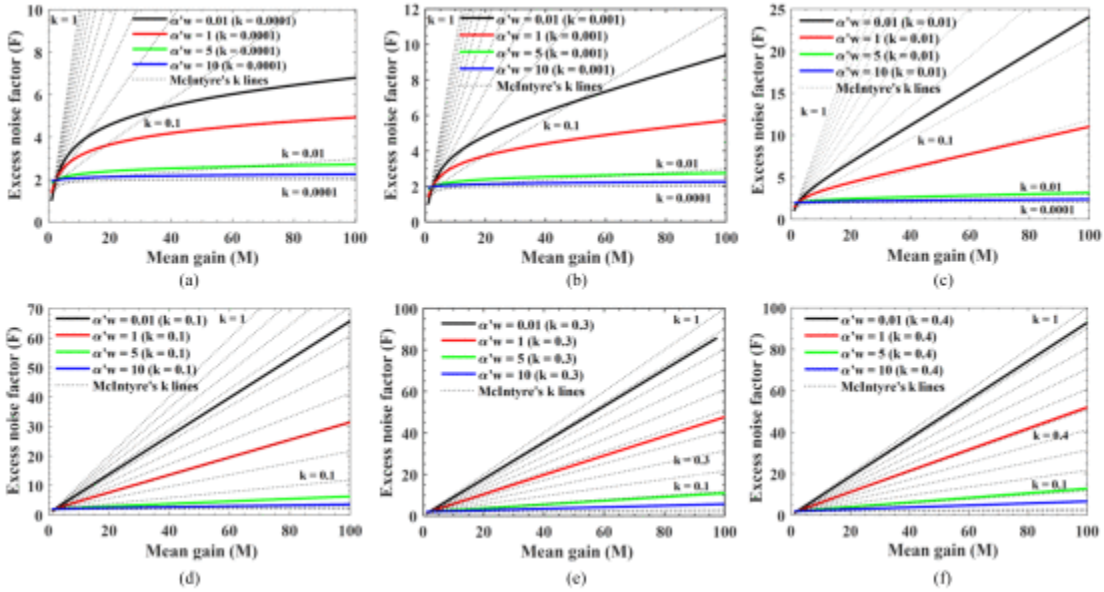

Fig. 3. Distributed-injection excess-noise factor (Fa) as a function of distributed-injection mean gain (Ma) for different absorption profiles with an exponential decay function. Six cases of hole-to-electron ionization coefficient ratio (*k*) are considered. The *k* values are 0.0001, 0.001, 0.01, 0.1, 0.3 and 0.4. In addition, McIntyre's *k* (β/α) lines (i.e., *x*/*w* = 0) are shown using the dotted lines: 0.0001, 0.001, 0.01 and 0.1 to 1 with an increment of 0.1.

Fig. 3 shows that excess noise factor increases with the narrow to flat absorption profile. For example, F_a increases by a factor of 2.35 at $M_a = 20$ for *k* = 0.0001 when a very narrow absorption profile ($\alpha' = 10$) is replaced by a nearly flat profile ($\alpha' = 0.01$). In addition, even when *k* is very low (~0.0001), F_a begins to increase dramatically beyond a certain threshold value of $M_a = 2.5$ if mixed injection is allowed—a behavior that is very different from that seen in the case of edge injection. Moreover, the mean gain threshold at which F_a becomes large is governed by the absorption profile and *k*. Additionally, for a particular *k* value, the shape of the distributed F_a versus the distributed M_a is now very different from what McIntyre formula predicts, as shown in Fig. 3.

Overall, McIntyre's *F* either underestimates or overestimates the distributed F_a, depending on the photon-absorption profile and value of *k*. For example, as shown in Fig. 3(a), McIntyre's *F* at *M* = 20 with low value of *k* (~0.0001), underestimates the distributed F_a by the factors of 0.92, 0.81, 0.53, and 0.42 for narrow to nearly flat absorption profiles with α' values of 10, 5, 1, and 0.01, respectively. However, for high value of *k* (*k* =

0.1 in Fig. 3(d)), McIntyre's *F* at *M* = 20 overestimates the distributed F_a by the factors of 1.29 and 1.61 for the narrow absorption profiles with α' values of 5 and 10, respectively. At the same time, for broader absorption profiles associated with the same *k* value of 0.1, McIntyre's *F* at *M* = 20 underestimates the distributed F_a by the factors of 0.5 and 0.26 for α' values of 1 and 0.01, respectively. Note that the small values of *k* of 0.01 or lower are important from a practical standpoint as there are several bulk materials that exhibit this type of behavior, including Si [4], [5] InAs [6], and AlAsSb [7]. In addition, high values of *k* (>0.1) are also important for submicron multiplication regions (e.g., Si *pn*-junction APDs), where the very high electric fields (>255 kV/cm) cause an increase in the *k* value [8], [9]. For example, the value of *k* for a *p*-*n* junction Si APD for typical operation is in the range of 0.1 – 0.56 for the high field values in the range of 255 – 900 kV/cm [9]. As seen from Fig. 3(f), for high values of *k*(~0.4), F_a exhibits a dramatic increase (by a factor of 6.6 at $M_a = 20$) from a narrow absorption profile (α' = 10) to a nearly flat profile (α' = 0.01). Such increase is very dramatic for a *k* value of 0.4, as compared to an increase by a factor of 2.35 for a low *k*value of 0.0001 with similar absorption profiles.

In summary, our analytical results indicate that McIntyre's edge-injection formula for *F*may either underestimate or overestimate the distributed-injection F_a, depending on the photon-absorption profile and the value of *k*. Hence, usage of both *k* and the photon-absorption distribution profile in the distributed injection formula for F_a can be critical in the reliable prediction of *F* in many real devices that involve mixed injection.

SECTION IV. Experimental Validation of the Theory

McIntyre's edge-injection formula for *F* can be inaccurate when applied to APDs with submicron multiplication region widths (e.g., <500 nm) and high values of *k* (e.g., >0.12) [4] [Si], [8], [9][Si], [11][GaAs], [12][Si]. One of the main reasons for such inaccuracy is the presence of mixed injection. For example, McIntyre's formula for *F* overestimated the measured *F* (at 830 nm excitation with *k* = 0.12) for a n^+-*p*-*π*-p^+ reach-through Si APD [4]. Other examples are low-noise CMOS APDs with a 470 nm multiplication region width [8] designed for the 380 nm and 600 nm excitations. For these devices, it was shown that McIntyre's *F* significantly overestimated the measured *F* for a high value of *k* (~1). In this case, the prediction error was attributed to a combination of the distributed carrier injection and the dead-space effect in the thin multiplication region [8].

Recently, the authors have reported calculated and measured excess noise factors for a speed-optimized, large area N-well/P-sub APD, which was fabricated in 0.13-µm CMOS process [9]. Here, too, *F* deviated from that provided by McIntyre's classical excess-noise formula. To obtain an accurate prediction of *F*, the authors resorted to calculating *F* using wavelength-dependent DSMT model under mixed-injection with an extensive numerical method [9]. Specifically, in addition to accounting for the electron-initiated avalanche multiplication process, hole injection and mixed-carrier injection were also taken into account in the recursive DSMT model to calculate *M* and *F* numerically while taking into account the absorption profile of N-well/P-sub CMOS APD [9]. The excess noise factor for this device was calculated using non-local Si ionization coefficients, and the results are shown in Fig. 4 (reproduced from [9]) with a dash-dot line.

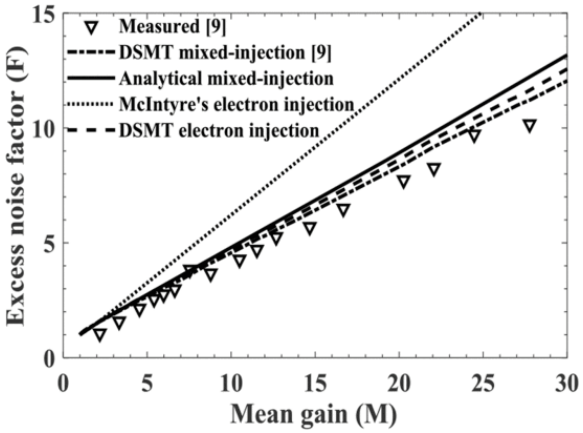

Fig. 4. Distributed-injection excess-noise factor (Fa) as a function of distributed-injection mean gain (Ma) for the N-well/P-sub CMOS APD. The triangles are the measured values reproduced from [9]using a 633 nm He-Ne laser. The solid and dotted lines indicate calculated results using exact analytical formulas under total mixed-injection and edge-electron injection respectively.

Here we use our derived exact analytical formula for F_a under distributed injection with zero dead space to determine *F* for the N-well/P-sub APD and compare to the measured *F*, as shown in Fig. 4. The triangles are the measured values of *F* reproduced from [9]using a 633 nm He-Ne laser. The excess noise factor is calculated using the exact analytical formula under total mixed-injection (electron, hole and distributed injection) while taking into account local ionization coefficients of Si [21]; the results are shown in the figure by the solid line. The calculation is based on using equations (4) and (8) in [9], except that we use our analytical expressions developed in this paper with zero dead space. The *k* value was calculated to be approximately 0.4. Note that the value of *k* for silicon is much larger at very high electric fields present in very thin multiplication regions (e.g., <400 nm [22]–[23][24][25][26][27] than that for bulk silicon) as shown in Fig. 1 in [28]. Fig. 4 shows that the calculated *F* (solid line) are in good agreement with the measured values for the N-well/P-sub APD.

The calculated *F* using McIntyre's edge-injection formula is shown in Fig. 4 by the dotted line. The comparison between the excess-noise factors corresponding to McIntyre's formula (edge electron injection) and our analytical mixed-injection formula shows that McIntyre's prediction of *F* overestimates both the measured and the calculated total mixed-injection *F.* This is also evident from Fig. 3(f), where McIntyre's *F* (for a *k* value of 0.4) overestimates the distributed F_a for narrow absorption profiles (e.g., α' = 5 and 10). In addition, the calculated *F* using the DSMT model for edge electron injection is shown in Fig. 4 by the dash line. (The *k* value turns out to be approximately 0.4). Note that the calculated *F* for both the analytical and numerical cases are slightly higher than the measured values. This could be due to the presence of non-uniform electric fields in the multiplication region of N-well/P-sub APD [9]. Additionally, dead space, which is ignored in the mixed/distributed injection formulas in this paper, also plays an important role to calculate *F* numerically with accuracy for a thin multiplication region of 270 nm for the N-well/P-sub APD as shown in [9]. This is why the DSMT (edge-/mixed-injection) is showing better agreement with measurements than that produced by the closed-form edge-injection/distributed-injection formulas; nonetheless, the latter offers a drastic computational simplification compared to the DSMT method. In addition, dead space has a dominant effect on calculating *F* using the DSMT as compared to edge-/distributed- injection for the thin N-well/P-sub APD considered here. Moreover, the calculated *F* using the simplified closed-form formulas show that distributed injection provides improved agreement with measurements as compared to the edge-electron injection formula for *F*.

SECTION V. Conclusion

Exact and easy-to-use analytical formulas for the excess noise factor are derived for mixed carrier injection and distributed-carrier injection APDs as shown in (21) and (29), respectively. It is our belief that the rigorous probabilistic derivation given here to obtain (21) is both simpler to follow and more direct than the McIntyre's equation (4) in [15], following (13) in [2], using a different and restricted technique. The analytical results are in excellent agreement with those calculated using the exact, numerically implemented DSMT method [10]. The results are also in good agreement with experiments [9]. The newly-derived formulas reveal that in contrast to the case of edge electron injection, even with a small level of hole ionization (e.g., small $k \sim 0.0001$), the excess noise behavior exhibits a dramatic increase when mixed injection is allowed. It is also shown that the distributed-injection excess noise factor increases relative to the predictions offered by the classical McIntyre's theory, which assumes edge injection, depending on the absorption profile as it ranges from narrow to flat within the multiplication region. Comparisons show that McIntyre's predictions of the excess noise factor either underestimate or overestimate the distributed-injection F_a, depending on the photon absorption profile and the value of k. Hence, relying on the k value alone in predicting the excess noise factor can be very misleading in cases when mixed injection is occurring. Therefore, the simple formulas reported in this paper provide a valuable tool for optimizing the design of APD structures that exhibit even small levels of photon absorption in their multiplication regions.

Acknowledgment

The authors would like to thank P. Das and M. R. Hasan for their helpful support.

References

1. G. P. Agrawal, Fiber-Optic Communication Systems, Hoboken, NJ, USA:Wiley, 2012.

2. R. J. McIntyre, "Multiplication noise in uniform avalanche diodes", *IEEE Trans. Electron Devices*, vol. ED-13, no. 1, pp. 164-168, Jan. 1966.

3. P. P. Webb, R. J. McIntyre, J. Conradi, "Properties of avalanche photodiodes", *RCA Rev*, vol. 35, pp. 234-278, Jun. 1974.

4. T. Kaneda, H. Matsumoto, T. Sakurai, T. Yamaoka, "Excess noise in silicon avalanche photodiodes", *J. Appl. Phys.*, vol. 47, no. 4, pp. 1605-1607, Apr. 1976.

5. C. H. Tan, J. P. R. David, G. J. Rees, R. C. Tozer, D. C. Herbert, "Treatment of soft threshold in impact ionization", *J. Appl. Phys.*, vol. 90, pp. 2538-2543, Sep. 2001.

6. G. Satyanadh, R. P. Joshi, N. Abedin, U. Singh, "Monte Carlo calculation of electron drift characteristics and avalanche noise in bulk InAs", *J. Appl. Phys.*, vol. 91, no. 3, pp. 1331-1338, Feb. 2002.

7. X. Yi et al., " Demonstration of large ionization coefficient ratio in AlAs 0.56 Sb 0.44 lattice matched to InP ", *Sci. Rep.*, vol. 8, Jun. 2018.

8. A. Pauchard, P. Besse, R. Popovic, "Dead space effect on the wavelength dependence of gain and noise in avalanche photodiodes", *IEEE Trans. Electron Devices*, vol. 47, no. 9, pp. 1685-1693, Sep. 2000.

9. M. M. Hossain et al., "Low-noise speed-optimized large area CMOS avalanche photodetector for visible light communication", *J. Lightw. Technol*, vol. 35, no. 11, pp. 2315-2324, Jun. 2017.

10. M. M. Hayat, B. E. A. Saleh, M. C. Teich, "Effect of dead space on gain and noise of double-carrier-multiplication avalanche photodiodes", *IEEE Trans. Electron Devices*, vol. 39, no. 3, pp. 546-552, Mar. 1992.

11. K. F. Li et al., "Avalanche noise characteristics of thin GaAs structures with distributed carrier generation [APDs]", *IEEE Trans. Electron Devices*, vol. 47, no. 5, pp. 910-914, May 2000.

12. C. H. Tan et al., " Avalanche noise measurement in thin Si p + - i-n + diodes ", *Appl. Phys. Lett.*, vol. 76, no. 26, pp. 3926-3928, Jun. 2000.

13. T. Bendib, L. Pancheri, F. Djeffal, G.-F. Dalla Betta, "Impact of temperature and doping concentration on avalanche photodiode characteristics", *Proc. World Congr. Eng.*, vol. I, pp. 5-8, Jul. 2–4, 2014.
14. M. M. Hayat, Z. Chen, M. A. Karim, "An analytical approximation for the excess noise factor of avalanche photodiodes with dead space", *IEEE Electron Device Lett.*, vol. 20, no. 7, pp. 344-347, Jul. 1999.
15. R. J. McIntyre, "A new look at impact ionization—Part I: A theory of gain noise breakdown probability and frequency Response", *IEEE Trans. Electron Devices*, vol. 46, no. 8, pp. 1623-1631, Aug. 1999.
16. P. Yuan et al., "Impact ionization characteristics of III–V semiconductors for a wide range of multiplication region thicknesses", *IEEE J. Quantum Electron.*, vol. 36, no. 2, pp. 198-204, Feb. 2000.
17. M. A. Saleh et al., "Impact-ionization and noise characteristics of thin III–V avalanche photodiodes", *IEEE Trans. Electron Devices*, vol. 48, no. 12, pp. 2722-2731, Dec. 2001.
18. J. S. Cheong, M. M. Hayat, X. Zhou, J. P. R. David, "Relating the experimental ionization coefficients in semiconductors to the nonlocal ionization coefficients", *IEEE Trans. Electron Devices*, vol. 62, no. 6, pp. 1946-1952, Jun. 2015.
19. A. G. Chynoweth, "Ionization rates for electrons and holes in silicon", *Phys. Rev.*, vol. 109, no. 5, pp. 1537-1540, Mar. 1958.
20. M. C. Teich, K. Matsuo, B. E. A. Saleh, "Excess noise factors for conventional and superlattice avalanche photodiodes and photomultiplier tubes", *IEEE J. Quantum Electron.*, vol. QE-22, no. 8, pp. 1184-1193, Aug. 1986.
21. R. Van Overstraeten, H. D. Man, "Measurement of the ionization rates in diffused silicon p-n junctions", *Solid State Electron*, vol. 13, no. 5, pp. 583-608, May 1970.
22. M. M. Hossain, J. Ghasemi, P. Zarkesh-Ha, M. M. Hayat, "Design modeling and fabrication of a CMOS compatible p-n junction avalanche photodiode", *Proc. 26th IEEE Photon. Conf.*, pp. 584-585, Sep. 8–12, 2013.
23. S. Ray, M. M. Hella, M. M. Hossain, P. Zarkesh-Ha, M. M. Hayat, "Speed optimized large area avalanche photodetector in standard CMOS technology for visible light communication", *Proc. 13th IEEE Sensors*, pp. 2147-2150, Nov. 3–5, 2014.
24. M. M. Hossain, P. Zarkesh-Ha, J. P. R. David, M. M. Hayat, "Low breakdown voltage CMOS compatible p-n junction avalanche photodiode", *Proc. 27th IEEE Photon. Conf.*, pp. 170-171, Oct. 12–16, 2014.
25. M. M. Hossain, P. Zarkesh-Ha, M. M. Hayat, "Linear mode CMOS compatible p-n junction avalanche photodiode with operating voltage below 9 V", *Proc. 28th IEEE Photon. Conf.*, pp. 436-437, Oct. 4–8, 2015.
26. M. M. Hossain, "Linear mode CMOS compatible p-n junction avalanche photodiode for smart-lighting applications", Aug. 2015, [online] Available: http://digitalrepository.unm.edu/ose_etds/8/.
27. M. M. Hossain, M. M. Hayat, "High responsivity double-junction CMOS-compatible avalanche photodiode", *Proc. 29th IEEE Photon. Conf.*, pp. 262-263, Oct. 2–6, 2016.
28. E. Jamil, J. S. Cheong, J. P. R. David, M. M. Hayat, "On the analytical formulation of excess noise in avalanche photodiodes with dead space", *Opt. Exp.*, vol. 24, no. 19, pp. 21597-21608, Sep. 2016.